

Orthogonal Arrays in Normal and Injured Respiratory Airway Epithelium

RONALD E. GORDON

Department of Pathology, Mount Sinai School of Medicine of the City University of New York, New York 10029

ABSTRACT Orthogonal arrays are found on plasma membranes of glial cells, in the central nervous system, on muscle plasma membranes at neuromuscular junctions, and on a variety of epithelial cells. These structures have been correlated with ion flux. With the aid of freeze fracture technique, orthogonal particle arrays were found on plasma membranes on airway epithelial cells of rats and hamsters. They have been found in abundance at the base of secretory cells throughout normal airway epithelium. These structures were found to increase in number during regeneration in response to injury and they were found in great numbers on plasma membranes of all airway cells in response to acute and chronic NO₂ exposure. The lateral and basal plasma membranes of the respiratory epithelium are a new source for studying orthogonal arrays. The normal number and distribution of these arrays can be perturbed in response to mechanical and chemical injury.

Orthogonal particle assemblies (rectangular arrays) are closely packed 6-nm intramembrane particles arranged in a square lattice. These assemblies have been found on the P-face of freeze-fractured plasma membranes of a variety of cells (1–11). Mammalian astrocytes, in particular, can be identified in freeze fractures by the abundance of these structures on their plasma membrane (12).

The biochemical nature of these particles and their function in the membrane have not been determined. It has been speculated that these structures are associated with ion flux, at least in astrocytes (13).

In this report we describe a rich source for these orthogonal structures in respiratory epithelium of rats and hamsters. We also describe conditions that increase their abundance, thereby perhaps providing a mechanism whereby these structures could be biochemically characterized and their function determined.

MATERIALS AND METHODS

20 male Syrian Golden hamsters weighing ~60 g for the chronic study and 125 g for the acute study were divided into two groups. One group of eight animals was exposed to NO₂: 2 for 6 h, 2 for 24 h, 2 for 48 h, and the last 2 remained as controls breathing room air. The second group of 12 animals was exposed to NO₂: 2 for 1 mo, 2 for 5 mo, 2 for 9 mo, and the remaining six animals were used as unexposed age controls, two animals corresponding to each exposure period (1, 5, and 9 mo).

Rationale for NO₂ Exposure: NO₂ is a noxious gas that has been known to cause emphysematous lesions in rats (14) and hamsters (15). We have been using continuous NO₂ exposure in hamsters as an animal model for the study of the development and progression of lesions caused by this agent in bronchioles and alveolar epithelium. During the studies in which we exam-

ined barrier function disruption of respiratory epithelium we made the observations reported in this manuscript.

NO₂ Exposure Techniques: The exposure groups were treated with NO₂ at concentrations of 30 ppm for 22 h per day, 7 d per wk. 30 ppm was chosen because it was low enough not to cause death and yet high enough to cause a consistent lesion where lower levels do not. The NO₂ exposed hamsters were housed separately in stainless steel cages according to the method of Kleinerman et al. (16). The NO₂ was generated by passing dry N₂ through ice-cooled NO₂. The airflow in the chambers was controlled by an exhaust pump that generated a negative pressure of 2 cm H₂O. NO₂ concentration was monitored by an in line Columbia Scientific Industries CSI 1600 NO₂ (Columbia Scientific Industries, Corp., Austin, TX) analyzer and continuously recorded on a Brown-Honeywell recorder (Honeywell, Inc., Minneapolis, MN). The NO₂ analyzer was calibrated and the chambers intermittently checked by the method of Saltzman (17).

Tissue Preparation: At the prescribed times of sacrifice, the animals were anesthetized lightly with an intraperitoneal injection of 0.75 ml of a 1:1 dilution of sodium pentobarbital and exsanguinated via the abdominal aorta. The chest cavity was opened exposing the lungs and trachea. The lungs, trachea, and esophagus were carefully dissected from the chest cavity to avoid pleural perforation. The trachea was freed by an incision just above the larynx. The lungs were inflation-fixed via tracheal cannulation at 20 cm H₂O pressure for 3 h with a solution containing 3% glutaraldehyde and 0.2 M Na cacodylate, buffered at pH 7.4. The bronchioles and surrounding alveoli were dissected out and prepared for freeze fracture.

Freeze Fracture: Tissue cubes containing cross-sectional areas of bronchi and/or bronchioles were obtained as described above. These blocks were transferred from cold cacodylate buffer to a 25% glycerine/cacodylate buffer at 4°C. Glycerination proceeded for 90 min with gentle agitation every 15 min. Tissue blocks were then transferred to nickel-gold specimen holders and rapidly frozen between Balzers double-replica supports by immersion in Freon 22, cooled with liquid nitrogen. Frozen specimens were transferred to a precooled stage of the Balzers 301 freeze-fracture plant (Hudson, NH). Vacuum was increased to 10⁻⁶ torr. Lung tissue samples were fractured at a stage temperature of -110°C. Within 1 s following fracture, the specimens were shadowed with platinum-carbon at 45°C and carbon at 90°C. Freeze fracture replicas were

removed, lung tissue was digested from the replicas by successive washings in increasing concentrations of sodium hypochlorite, rinsed in three changes of triple-distilled filtered water, and mounted on 300-mesh copper grids.

All replicas were examined and photographed in a JEM 100CX electron microscope equipped with a goniometer stage. The lungs from each animal were coded by technician to prevent bias by the investigator and only after all statistical analyses were calculated was the data decoded. Each lung was evaluated independently and a minimum of five bronchioles from each animal were freeze fractured. The plasma membranes of at least 20 epithelial cells from each fracture were randomly photographed at 20,000 diameters magnification. A total of at least 100 micrographs at a final magnification of 60,000 diameters were morphometrically evaluated by counting the number of orthogonal arrays in each micrograph. The plasma membrane P face area was determined with the aid of a Numonics graphic calculator (Numonics Corp., Lansdale, PA). The number of arrays and surface area for each bronchiole was totaled and expressed as orthogonal arrays per square micrometer. The mean for each lung was calculated and compared with the other lung in each group and with its respective control by the Student's *t* test analysis.

RESULTS

Freeze fracture replicas of upper airways of rats involved in regeneration in response to mild mechanical injury show large

numbers of these orthogonal arrays in plasma membranes at the basal aspects of secretory and ciliated cells and on plasma membranes of basal cells. These structures were observed in the normal epithelium, but, they were few in number. This observation was an incidental finding in a previous report focused on changes in gap junctions (18). These rectangular particle aggregates were also observed as previously reported (19) on the basal aspects of plasma membranes of Clara cells from bronchioles of hamster lung. More recently, we have found that these structures were in abundance all over non-ciliated and ciliated cell plasma membranes of bronchioles in hamsters exposed to NO₂ briefly (6 to 48 h) or for long periods (1, 5, or 9 mo) (Fig. 1) as compared with controls (Fig. 2). Statistical analysis (Table I) indicated that there was no significant difference between animals within each group and also between NO₂ exposure groups or between control groups. As seen in Table I the lateral plasma membranes of bronchiolar epithelial cells exposed to NO₂ demonstrated a significant increase over the plasma membranes from lungs of unexposed age control animals.

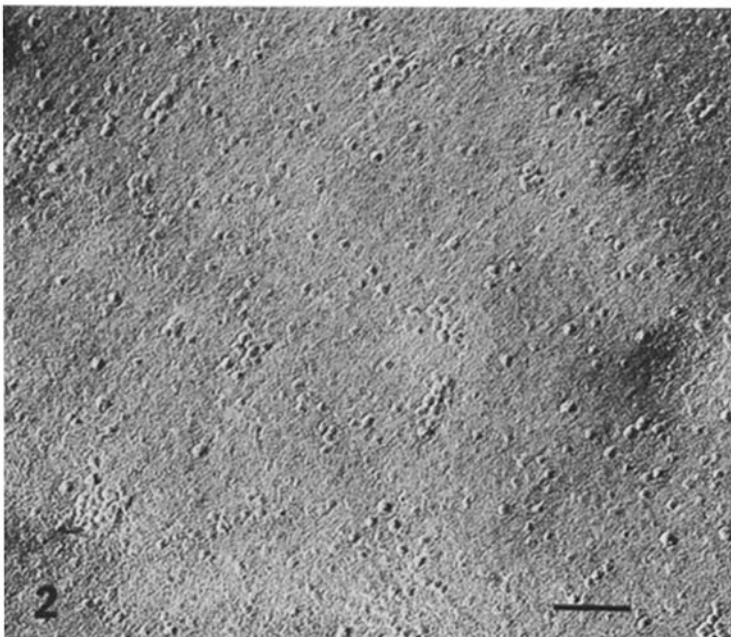
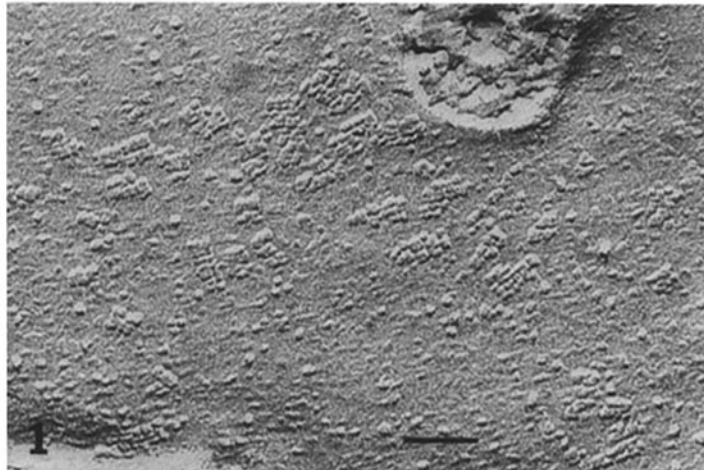


FIGURE 1 and 2 Fig. 1: Transmission electron micrograph of a freeze fracture replica of the lateral surface of a bronchiolar epithelial Clara cell that had been fixed after 5 mo continuous NO₂ exposure. Many orthogonal arrays composed of 6-nm particles can be seen (arrow). Fig. 2: Transmission electron micrograph of a freeze fracture replica of the lateral surface of an unexposed control bronchiolar epithelial Clara Cell. Orthogonal arrays were less dense and the number of particles in each assembly is reduced. Bars, 86 nm. × 132,000.

TABLE I
Number of Arrays per Square Micrometer for Each Exposure Period \pm SE

	Animal	6 h	24 h	48 h	1 mo	5 mo	9 mo
Control	1	10.2 \pm 0.97	10.2 \pm 0.97	10.2 \pm 0.97	9.8 \pm 1.33	10.9 \pm 1.41	10.6 \pm 0.99
	2	10.4 \pm 1.29	10.4 \pm 1.29	10.4 \pm 1.29	10.1 \pm 1.22	11.2 \pm 1.12	10.2 \pm 1.04
NO ₂	1	44.4 \pm 2.84	45.0 \pm 3.21	51.6 \pm 3.28	45.0 \pm 2.02	42.8 \pm 2.08	41.8 \pm 2.50
	2	42.2 \pm 5.01	49.0 \pm 3.32	45.4 \pm 3.49	41.8 \pm 1.93	42.0 \pm 1.67	45.0 \pm 2.30

$P > 0.001$ between NO₂ and control animals.

DISCUSSION

Orthogonal arrays have been found in a variety of cell types. They have been most commonly found in and around nervous tissue. This includes Mueller cells of the retina (4) glial cells of the central nervous system (3, 13, 20, 21) and on skeletal muscle plasma membranes, especially at non-neuromuscular junctional regions in mammals (20–22). However, Heuser et al. (23) in amphibia also observed orthogonal arrays at the neuromuscular junction. They have been found on plasma membranes of many epithelial cells including hepatocytes (5), intestine (6, 7), regenerating trachea (18), bronchioles (19), and kidney-collecting tubules (8).

The increase in orthogonal arrays was observed as early as 6 h after initiation of NO₂ exposure. It would be important to know whether the increase in arrays was due to reorganization of pre-existing plasma membrane particles or insertion of the molecules from either a cytoplasmic pool or de novo protein synthesis. The data in this report can not directly support any specific mechanism of formation. However, it could be suggested that the significant increase was due to newly inserted or synthesized molecules since the density of these particles in control plasma membranes, based on qualitative assessment would not be adequate for the observed increase in particle arrays. If this suggestion is verified, this system would be excellent for studying the biochemistry of these molecules and isolation of their specific polyribosomes and mRNAs.

Orthogonal arrays have been observed over the entire surface of glial cells, but they are most prevalent on "end feet" and adjacent to an extended space (i.e., perivascular submeningeal or sinusoidal) or to a fluid system (i.e., blood, lymph, or cerebrospinal fluid) (13). Similarly, these arrays on epithelial membranes are found near periglandular spaces and adjacent to basal lamina or fluid spaces (5–9). It has been suggested, based on their location, that these structures are associated with or play a role in the regulation of the concentration of certain ionic species in the interstitial fluids (13). Further, these particle arrays may represent ionic leakage sites, specialized for the relocation of ions away from active regions (13). Rash and Elisman (22) Elisman et al. (24, 25) have called attention to the relative K⁺ flux and of Ca²⁺-ATPase.

It has recently been shown that ionic pumping and transport, particularly of sodium, potassium, calcium, and chloride is an active process in the respiratory epithelium (26). The presence of orthogonal arrays at the cell base of the normal airway epithelium may be responsible for normal ion flux. Conditions of stress, such as anoxia, affect ion flux (26). It has not been determined if NO₂, which also stresses the epithelium, has an effect on ion flux. However, NO₂ exposure increases the abundance of orthogonal arrays. The increase in

these arrays may be involved in ion fluxes in this tissue and increased numbers of arrays may correspond to altered ion fluxes observed. It is clear that these structures may be critical to the normal function of airway epithelium and disruption of these structures may dramatically affect epithelial cell function.

The author thanks Dr. Michael L. Marin for his assistance with the freeze fracture techniques and his acute observations in our previous work leading to current observations. In addition, he is also grateful to Maria E. Becerril for typing the manuscript.

This work was supported by grants HL-26293 and HL-25766 from the National Institutes of Health.

Received for publication 2 July 1984, and in revised form 12 October 1984.

REFERENCES

- Dreifuss, J. J., C. Sandri, K. Akert, and H. Moor. 1975. Intercellular junctions between pituitary cells. A freeze-fracture study. *Experientia*. 31:737.
- Dreifuss, J. J., C. Sandri, K. Akert, and H. Moor. 1975. Ultrastructural evidence for sinusoidal spaces and coupling between pituitary cells in the rat. 161:33–45.
- Landis, D. M. D., and T. S. Reese. 1974. Arrays of particles in freeze-fractured astrocytic membranes. *J. Cell Biol.* 60:316–320.
- Reale, E., and E. Luciano. 1974. Introduction to freeze-fracture method in retinal research. *Albrecht von Graefes Arch. Klin. Exp. Ophthalmol.* 192:73–87.
- Kreutziger, G. O. 1968. Freeze-etching of intercellular junctions in mouse liver. In Proceedings of the 26th Meeting of the Electron Microscope Society of America, Claitors Publishing Division, Baton Rouge. p. 234–235.
- Bordin, C., and A. Perrelet. 1978. Orthogonal arrays of particles in plasma membranes of the gastric parietal cell. *Anat. Rec.* 192:297–304.
- Stachelin, L. A. 1972. Three types of gap junctions interconnecting intestinal epithelial cells visualized by freeze-etching. *Proc. Natl. Acad. Sci. USA.* 69:1318–1321.
- Humbert, F., C. Pricam, A. Perrelet, and L. Orci. 1975. Specific plasma membrane differentiation in the cells of the kidney collecting tubule. *J. Ultrastruct. Res.* 52:13–20.
- Inoue, S., and J. C. Hogg. 1977. Freeze-etch study of the tracheal epithelium of normal guinea pigs with particular reference to intercellular junctions. *J. Ultrastruct. Res.* 61:89–99.
- Wekerle, H., U.-P. Ketelsen, and M. Erast. 1980. Thymic nurse cells lymphoepithelial complexes in murine thymuses. Morphological and serological characterization. *J. Exp. Med.* 151:925–944.
- Rash, J. E., L. A. Stachelin, and M. H. Ellisman. 1974. Rectangular arrays of particles in freeze-cleaved plasma membranes are not gap junctions. *Exp. Cell Res.* 86:187–190.
- Massa, P. T., and C. C. Magnaini. 1982. Cell junctions and intramembrane particles of astrocytes and oligodendrocytes. A freeze-fracture study. *Neuroscience*. 7:523–538.
- Hatton, J. D., and M. H. Elisman. 1981. The distribution of orthogonal arrays and their relationship to intercellular junctions in neuroglia of the freeze-fractured hypothalamo-neurohypophysial system. *Cell Tissue Res.* 215:309–323.
- Freeman, G., and G. B. Haydon. 1964. Emphysema after low-level exposures to nitrogen dioxide. *Arch. Environ. Health.* 8:125–128.
- Kleinerman, J., and D. E. Niewoehner. 1973. Physiological, pathological and morphometric studies of long-term nitrogen dioxide exposure and recovery in hamsters. *Am. Rev. Respir. Dis.* 107:1081–1091.
- Kleinerman, J., and D. Rynbrandt. 1976. Lung proteolytic activity and serum protease inhibition after nitrogen dioxide exposure. *Arch. Environ. Health.* 31:37–41.
- Saltzman, B. E. 1954. Colorimetric microdetermination of NO₂ in the atmosphere. *Anal. Chem.* 26:1949–55.
- Gordon, R. E., B. P. Lane, and M. Marin. 1982. Cycle specific formation of gap junctions in regenerating rat tracheal epithelium. *Exp. Lung Res.* 3:47–56.
- Marin, M. L., R. E. Gordon, B. W. Case, and J. Kleinerman. 1982. Ultrastructure of broncholar epithelium in freeze fracture replicas. *Lung.* 160:257–266.
- Anders, J. J., and M. W. Brightman. 1979. Assemblies of particles in the cell membranes of developing mature and reactive astrocytes. *J. Neurocytol.* 8:777–795.
- Elfvin, L. G., and C. Forsman. 1978. The ultrastructure of junctions between satellite cells in mammalian sympathetic ganglia as revealed by freeze-etching. *J. Ultrastruct. Res.* 63:261–274.
- Rash, J. E., and M. H. Ellisman. 1974. Studies of excitable membranes. I. Macromolecular specializations of the neuromuscular junctions and the nonjunctional sarcolemma.

- J. Cell Biol.* 63:567-580.
23. Heuser, J. E., F. S. Reese, and D. M. D. Landis. 1974. Functional changes in frog neuromuscular junctions studied with freeze-fracture. *J. Neurocytol.* 3:109-131.
 24. Ellisman, M. H., J. E. Rash, L. A. Staehelin, and K. R. Porter. 1976. Studies of excitable membranes. II. A comparison of specializations at neuromuscular junction and non-junctional sarcolemmas of mammalian fast and slow twitch muscle fibers. *J. Cell Biol.* 68:752-774.
 25. Ellisman, M. H., M. H. Brooke, K. K. Kaiser, and J. E. Rash. 1978. Appearance in slow muscle sarcolemma of specializations characteristic of fast muscle after reinnervation by a fast muscle nerve. *Exp. Neurol.* 58:59-67.
 26. Statts, M. J., J. T. Gatzky, and R. C. Boucher. 1984. Metabolic inhibition of bronchial ion transport. *Fed. Proc.* 43:829.